

---

School of Natural Sciences and Mathematics

---

2013-10-10

*Conductive Functional Biscrolled Polymer and  
Carbon Nanotube Yarns*

UTD AUTHOR(S): Marcio D. Lima and Ray H. Baughman

©2013 The Royal Society of Chemistry. This article may not be further made available or distributed.

## Conductive functional bicrolled polymer and carbon nanotube yarns

Cite this: *RSC Adv.*, 2013, **3**, 24028

Received 30th July 2013  
Accepted 10th October 2013

DOI: 10.1039/c3ra45558k

[www.rsc.org/advances](http://www.rsc.org/advances)

Shi Hyeong Kim,<sup>a</sup> Hyeon Jun Sim,<sup>a</sup> Min Kyoong Shin,<sup>a</sup> A Young Choi,<sup>b</sup> Youn Tae Kim,<sup>b</sup> Marcio D. Lima,<sup>c</sup> Ray H. Baughman<sup>c</sup> and Seon Jeong Kim<sup>\*a</sup>

Bicrolling aligned electrospun fiber (AEF) sheets and carbon nanotube (CNT) sheets were fabricated for conductive, functional yarns by a versatile dry composite method. Our bicrolling (twist-based spinning) method is based on spinnable polymer fiber sheets and spinnable CNT sheets unlike the previous bicrolling technique using unspinnable nanopowders and spinnable CNT sheets. The CNT sheet in composite yarns acted as effective electrical wires forming dual Archimedean multilayer rolled-up nanostructures. The weight percent of the electrospun polymer fibers in the composite yarns was over 98%, and the electrical conductivity values of the composite yarns was 3 orders higher than those of other non-conducting polymer/CNT composite fibers which were electrospun from polymer solutions containing similar loading of CNTs. We also demonstrate that bicrolled yarns having various structures can be fabricated from spinnable AEF sheets and spinnable CNT sheets.

Solution electrospinning is an electrostatic method for producing ultrathin, continuous polymer or composite fibers from polymer solutions or melts in high electric fields.<sup>1</sup> In electrospinning, an electrified jet is formed by the use of a high voltage between a syringe tip and a metal collector, and the jet is continuously stretched due to the electrostatic repulsions between surface charges induced on the liquid jet. Finally, solid fibers are deposited on the collector by fast evaporation of solvent. Fibers made by electrospinning have been applied in various fields such as tissue engineering,<sup>2</sup> solar cells,<sup>3</sup> catalysis,<sup>4</sup> filtration,<sup>5</sup> protective clothing,<sup>6</sup> environmental protection,<sup>7</sup> sensors,<sup>8</sup> electronics,<sup>9</sup> and optics.<sup>10</sup> This is mainly due to the large surface area to volume ratio, high aspect ratio, and unique physical or chemical properties of electrospun fibers.<sup>11</sup> For

convenience of applications, electrospun fibers have been fabricated as randomly oriented nonwoven sheets,<sup>12</sup> aligned sheets,<sup>13</sup> bundles,<sup>14</sup> and fibers deposited on patterned electrodes<sup>15</sup> through the control of electric fields and the modification of collector shapes.

Despite many advantages, because most electrospun polymer fibers are not conductive, their resistance to electrical current is very high. The low electrical conductivity of electrospun polymer fibers<sup>16</sup> can prohibit applications such as electrical sensors, electrically powered actuators, energy storage devices, and energy harvesting devices. Although conducting polymers such as polyaniline and polypyrrole without or with non-conducting polymers have been electrospun,<sup>17</sup> the brittle nature of conducting polymers<sup>18</sup> is a problem to be overcome. Thereby, for more broad applications based on functionality of non-conducting polymer fibers, it is necessary to render electrospun polymer fibers electrically conductive. Many researchers have developed conductive composite fibers by electrospinning a mixture of carbon nanomaterials (for example, carbon nanotubes and carbon black) and non-conducting polymers in solvents.<sup>19–21</sup> However, the composite fibers made by previous methods have distinct limitations in enhancement of electrical conductivity although the electrical percolation threshold was achieved with increasing loading of conductive fillers.<sup>22,23</sup> Although high electrical conductivity of electrospun composite fibers has been achieved for practical applications through excessive loading of carbon nanofillers (over 20 wt%),<sup>24</sup> this generally results in dramatic decrease in fiber elongation.<sup>25</sup> It is still challenge to make highly conductive polymer fibers maintaining their polymeric functionality.

Here, we report a versatile dry composite method for conductive, functional yarns by bicrolling aligned electrospun fiber (AEF) sheets and carbon nanotube (CNT) sheets. Our bicrolling (twist-based spinning) method is based on spinnable polymer fiber sheets and spinnable CNT sheets unlike the previous bicrolling technique using unspinnable nanopowders and spinnable CNT sheets.<sup>26</sup> The CNT sheet in composite yarns acted as effective electrical wires forming dual Archimedean

<sup>a</sup>Center for Bio-Artificial Muscle and Department of Biomedical Engineering, Hanyang University, Seoul 133-791, Korea. E-mail: [sjk@hanyang.ac.kr](mailto:sjk@hanyang.ac.kr)

<sup>b</sup>IT Fusion Technology Research Center and Department of IT Fusion Technology, Chosun University, Gwangju 501-759, Korea

<sup>c</sup>The Alan G. MacDiarmid NanoTech Institute, University of Texas at Dallas, Richardson, TX 75083, USA

multilayer rolled-up nanostructures. The weight percent of the electrospun polymer fibers in the composite yarns was over 98%, and the electrical conductivity values of the functional composite yarns was at least 3 order higher than those of other non-conducting polymer/CNT composite fibers which were electrospun from polymer solutions containing similar loading of CNTs. We also demonstrate that biscrolled yarns having various structures can be fabricated from spinnable AEF sheets and spinnable CNT sheets.

Recently, the biscrolling technique was developed to make composite yarns using unspinnable particles and spinnable CNT sheets.<sup>26</sup> The technique enables to produce strong, conductive, flexible, weavable, and durable yarns by twisting particles and CNT sheets because CNT sheets drawn from multiwalled nanotube forests have excellent electrical and mechanical properties (the densified sheet resistance in the aligned direction is  $\sim 600 \Omega \text{ sq}^{-1}$ , and a stack of densified sheets has specific tensile strength of  $\sim 465 \text{ MPa g}^{-1} \text{ cm}^{-3}$ ).<sup>27</sup> The group demonstrated that producing weavable yarns comprising up to 95 weight percent of unspinnable particle or nanofiber powders is possible and the powders remain highly functional even after biscrolling.<sup>26</sup>

Unlike the previous biscrolling demonstration based on unspinnable nanoparticle or nanofiber powders deposited on CNT sheets, we show fabrication of conductive, functional biscrolled composite yarns by twisting bilayer or multilayer structures consisting of spinnable AEF sheets and spinnable CNT sheets (Fig. 1). First, for producing AEF sheets, aligned fibers were suspended over the gap between metal electrodes (the gap is  $\sim 4 \text{ cm}$ ), in the vicinity of which an electric field induces orientation of flying fibers (Fig. 1a).<sup>28</sup> The width, length, and thickness of the prepared AEF sheet were  $\sim 2 \text{ cm}$ ,  $\sim 4 \text{ cm}$ , and  $\sim 300 \mu\text{m}$ , respectively (Fig. 1b). Second, CNT sheets consisting of aligned nanotubes were produced from spinnable multiwalled nanotube forests by a simple drawing method (Fig. 1c), and the sheets can be easily transferred to another substrate or suspended over the gap at freestanding state (Fig. 1d). The width and length of the CNT sheet used for biscrolling were  $\sim 1 \text{ cm}$  and  $\sim 4 \text{ cm}$ , respectively, and the layer number of the CNT sheet used for biscrolled yarns was usually three although we used one to five layer sheets for electrical conductivity

changes according to the layer number and CNT weight percents. Finally, bilayer structures were prepared by the attachment of the CNT sheets to the AEF sheets (for the same width of the AEF sheet and the CNT sheet, the wider AEF sheet was cut before twisting), and then the bilayer sheets were twisted by an electric motor shaft with a flat rectangular paddle until the inserted twist was  $\sim 1000$  turns per m (Fig. 1e). We used as-drawn CNT sheets without densification of sheets using solvent or gas. The as-drawn one layer CNT sheet is aerogel having density of  $\sim 1.5 \text{ mg cm}^{-3}$  and thickness of  $\sim 20 \mu\text{m}$ .<sup>27</sup> Because of the low density of the CNT sheet, the weight percent of the polymer fibers in the composite yarn was over 98%.

For analyzing the spinnability of sheets and the yarn structures, we twisted AEF sheets, CNT sheets, and bilayer AEF/CNT sheets. We have discovered that various biscrolled yarn structures such as Fermat, Archimedean, and dual-Archimedean are produced by changing AEF sheets condition (such as a density, alignment).<sup>26</sup> If AEF sheets, CNT sheets, and bilayer AEF/CNT sheets are symmetry stressed during twisting, dual-Archimedean structure of yarn was observed. Fig. 2a and b show polymer yarns twisted from AEF sheets and morphology of polymer yarns. The polymer yarns were made from various functional polymers such as SEBS (elastomer), PVDF-HFP (piezoelectric material), PU (shape memory polymer), and their shapes resembled each other. The average diameters of uniform SEBS, PVDF, and PU fibers composing the yarns were  $\sim 6 \mu\text{m}$ ,  $\sim 2.2 \mu\text{m}$ , and  $\sim 4.5 \mu\text{m}$ , respectively. If the electrospun polymer fibers can have moderate or high electrical conductivity maintaining their functionality, they would be applicable as high performance strain sensors, piezoelectric energy harvesters, and electrothermally powered actuators. Fig. 2d and e show CNT yarns twisted from CNT sheets and morphology of CNT yarns. The CNT yarns have been developed for actuators, reinforcing materials, and electronic textiles because of their high electrical conductivity and mechanical strength.<sup>29</sup> Although direct polymer infiltration of CNT yarns has been carried out,<sup>30</sup> the infiltrated composite yarns do not entirely highlight polymer functionality because of small loading of polymers. Fig. 2g and h show biscrolled yarns twisted from the bilayer sheets consisting of AEF sheets and CNT sheets. Because of the twist of two

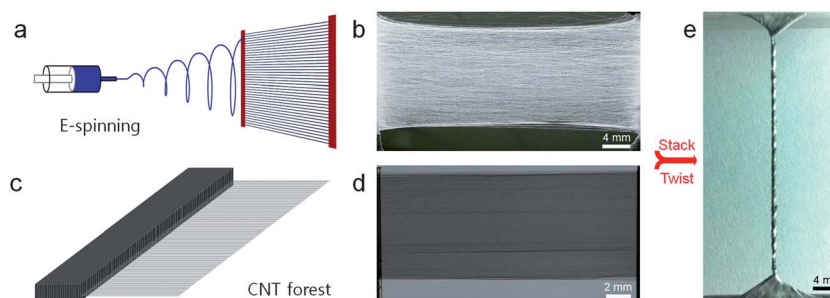


**Fig. 1** Biscrolling process using an aligned electrospun fiber (AEF) sheet and a CNT sheet. (a) Electrospinning of fibers from a polymer solution for producing an AEF sheet and (b) an optical photo image of the AEF sheet. Polymers used for the AEF sheet are SEBS (elastomer), PVDF-HFP (piezoelectric polymer), and PU (shape memory polymer). (c) Schematic showing a CNT sheet drawn from multiwalled nanotube forests and (d) an optical photo image of the CNT sheet. (e) Biscrolling of the AEF sheet and the CNT sheet, and an optical photo image of the biscrolled yarn with a barber-pole-type structure.

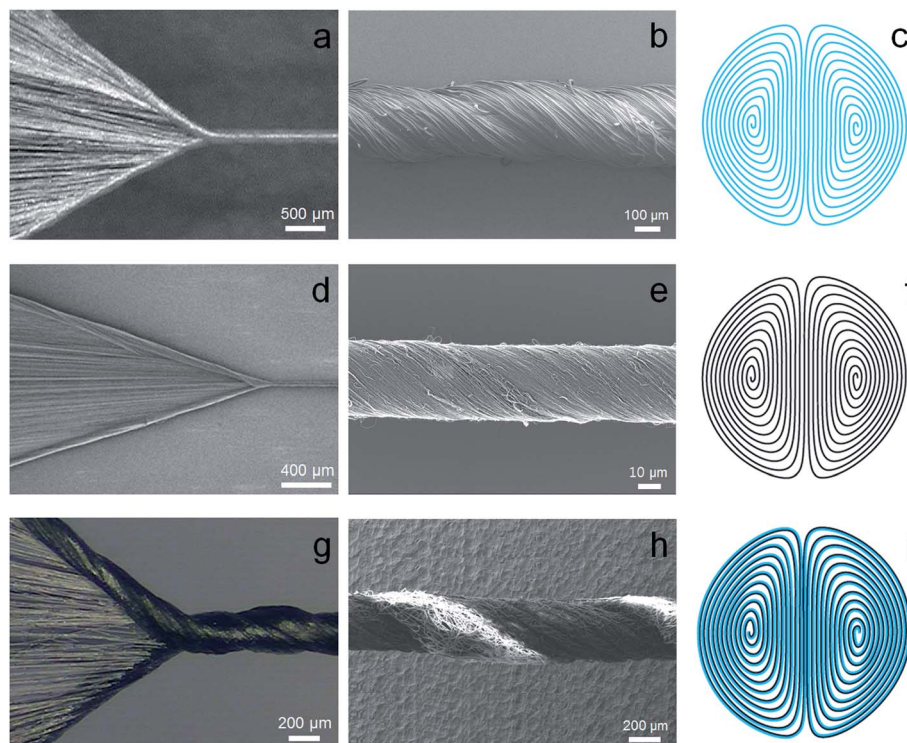


**Fig. 2** Yarn structures twisted from the AEF sheet, CNT sheet, and bilayer AEF/CNT sheets. (a–c) Yarn structures twisted from the spinnable AEF sheet: (a) a wedge shape formed during a spinning process, (b) SEM image of a polymer yarn, and (c) schematic showing a dual-Archimedean structure of the polymer yarn. (d–f) Yarn structures twisted from the spinnable CNT sheet: (d) a wedge shape formed during a spinning process, (e) SEM image of a CNT yarn, and (f) schematic showing a dual-Archimedean structure of the CNT yarn. (g–i) Yarn structures twisted from the bilayer AEF/CNT sheets: (g) a wedge shape formed during a spinning process, (h) SEM image of a biscrolled composite yarn, and (i) schematic showing a dual-Archimedean structure of the biscrolled composite yarn. Polymers used were SEBS (elastomer), PVDF-HFP (piezoelectric polymer), and PU (shape memory polymer). The layer number of CNT sheets used was three.

materials with different colors, white is the AEF sheet and black is CNT sheets, the biscrolled yarns had a barber-pole-type structure. Although the biscrolled yarns were made by a twist method, they maintained their scrolled shape at free-standing state because of van der Waals interactions between individual fibers with small diameters. Also, during biscrolling, CNTs can form good adhesion with polymer fibers by compressive forces. The electrical conductance of biscrolled yarn is same before scrolling bilayer. The CNT sheets in composite yarn are hardly damaged and acted as effective electrical wires forming dual Archimedean multilayer rolled-up nanostructures with small amount. Thereby, the biscrolled yarns consisting of CNT sheets and polymer fiber sheets can become a new composite material prepared by physical forces different from previous solution-based composite methods.<sup>31</sup> Another advantage of our method enables to maximize electrical properties of the composite by small loading of CNTs (below 2 wt%). Previous electrospun composite fibers achieved their high electrical conductivity by excessive loading of CNTs (over 10 wt%) in polymer solution.<sup>20</sup> The excessive loading of CNTs generally generates dramatic decrease of fiber elongation, and so the highly conductive composite fibers are often brittle. However, our suggestion can achieve high electrical conductivity by the control of CNT sheet numbers and the effective wiring by spiral nanostructures of continuous CNTs, maintaining mechanical properties of polymer fibers.

From the spinning wedge shape, we can identify the cross-section of yarns, as shown in Fig. 2c, f and i.<sup>26</sup> The sheet edges were buried in different interconnected scrolls, like in two dimensions for a Cornu spiral, and so the yarns can be named as dual-Archimedean scrolled. Because of well distributed dual-Archimedean structure of CNT sheets in the AEF length direction (Fig. 2g and i), the conductive path by CNT can contribute to high electrical conductivity despite very small loading of CNTs.

In Fig. 3, we present various structures of biscrolled yarns according to twisting techniques. In addition to biscrolled yarns with regular dual-Archimedean cross-sections (Fig. 2i), CNT-AEF-CNT or AEF-CNT-AEF multilayer scrolled yarns were fabricated (Fig. 3a and b). CNT-AEF-CNT multilayer scrolled yarns have CNT sheets exposed to outer surface of the yarn, whereas AEF-CNT-AEF multilayer scrolled yarns have AEF sheets exposed to outer surface of the yarn. We obtained biscrolled yarns with highly wrinkled CNT sheets by stretching AEF sheets before twisting (Fig. 3c and d). For the yarns, an AEF sheet (2 cm) was stretched up to 300% (for SEBS elastomer), and three layer CNT sheets were attached on the stretched AEF sheet, and then the two end tethered bilayer sheets were twisted until the inserted twist was  $\sim 250$  turns per m. In Fig. 3c, the biscrolled yarn was contracted up to  $\sim 40\%$  of the stretched AEF sheet length (8 cm) after twisting. In Fig. 3d, the biscrolled yarn was contracted up to  $\sim 40\%$  of the stretched AEF sheet length



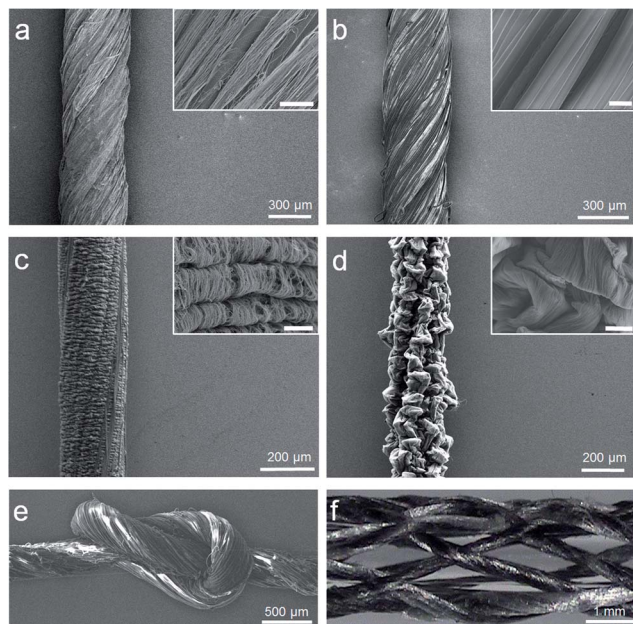


**Fig. 3** Various types of AEF/CNT composite yarns made by different sheet stacking and twisting technique. (a) SEM image of composite yarns fabricated by twisting CNT–AEF–CNT sheets. The inset shows CNTs exposed to the yarn surface. The inset scale bar is 10  $\mu\text{m}$ . (b) SEM image of composite yarns fabricated by twisting AEF–CNT–AEF sheets. The inset shows AEFs exposed to the yarn surface. The inset scale bar is 10  $\mu\text{m}$ . (c) SEM image of a AEF/CNT biscrolled yarn with periodically wrinkled CNT sheets. The inset shows a magnified image of the wrinkled CNT sheets. The inset scale bar is 20  $\mu\text{m}$ . (d) SEM image of a biscrolled yarn with irregularly wrinkled CNT sheets. The inset shows a magnified image of the wrinkled CNT sheets. The inset scale bar is 20  $\mu\text{m}$ . (e) SEM image of knotting biscrolled yarn. (f) SEM image showing braids consisting of 12 biscrolled yarns. The layer number of CNT sheets used was three. Polymers shown in (a), (b), (e) and (f) were SEBS, PVDF-HFP, and PU. Polymers shown in (c) and (d) were SEBS and PU.

(8 cm) during twisting unlike Fig. 3c. The difference of the contraction technique generated different wrinkle structures. In the case of shape memory polymer (PU), it was similar to fabricate wrinkled biscrolled yarn using an elastomer except for stretching the bilayer PU–AEF, twisting the bilayer PU–AEF/CNT, and contracting the PU–AEF/CNT biscrolled yarn at over glass transition temperature ( $\sim 60^\circ\text{C}$ ). Because weight percent of an AEF sheet in the composite yarns was over 98%, contraction of the wrinkled AEF/CNT biscrolled yarn was similar to that of an AEF scrolled yarn. The flexibility and durability of the biscrolled yarn enable to weave, knot the yarns, and braids consisting of 12 biscrolled yarns in Fig. 3e and f.

Fig. 4 shows electrical and mechanical properties of polymer yarns and twisted composite yarns with various structures. The weight percent of CNTs (three layer CNT sheets) in the twisted yarns was  $\sim 1.5\%$ . Actually, mechanical strength and elongation of the biscrolled composite yarns and the regular wrinkled biscrolled composite yarns having three layer CNT sheets were similar to those of the polymer yarns (Fig. 4a). However, electrical properties were highly enhanced as compared to polymer yarns and previous electrospun composite fibers with CNTs below  $\sim 5\text{ wt}\%$ . The change in resistance is different depending on the elongation of various structure of biscrolled yarns. Because of wrinkling structure of CNT sheets, the wrinkled

biscrolled yarns can be highly stretchable without large changes of electrical resistance as compared to regular biscrolled yarns made using the same materials. Various functional material and structures based conductive biscrolled composite yarns would be applicable as high performance strain sensors and stretchable electrodes. Fig. 4b shows typical  $I$ – $V$  characteristics for our composite yarns (three layer CNT sheets) with various structures shown in Fig. 2 and 3. The  $I$ – $V$  curves showed a linear ohmic behavior and the dc conductivity values of the composite yarns were of the order of  $10^2\text{ S m}^{-1}$ . The same value of resistance can be obtained regardless of the value of the applied voltage in the range of  $\pm 15\text{ V}$  (the inset of Fig. 4b). The electrical conductance was controllable according to different biscrolled yarn structures under the same loading of CNTs ( $\sim 1.5\text{ wt}\%$ ). For the similar yarn length and diameter, the wrinkled biscrolled yarns had higher electrical resistance than regular biscrolled yarns because the wrinkled biscrolled yarns were made from longer CNT sheets. Fig. 4c shows electrical conductivity with increasing CNT loading. Unlike general percolation threshold shown in conventional composites, our composite yarns possessed high electrical conductivity of  $\sim 140\text{ S m}^{-1}$  using a one layer CNT sheet (at  $0.5\text{ wt}\%$  CNT loading). Also, the biscrolled composite yarn presented linear increase in electrical conductivity with the increase of CNT weight. This means that electrical conductivity is proportionally controllable according to the layer number of CNT sheets. The conductivity values were higher at least three order than those of previous composite fibers containing similar CNT loading (Fig. 4d, literature data show electrical conductivity of electrospun nanocomposites with CNT weight content below  $5\%$ ).

In conclusion, we have suggested new dry composite methods based on aligned polymer fiber sheets made by electrospinning and CNT sheets drawn from multiwalled nanotube forests. Because both sheets were spinnable and a small amount of CNT sheets was loaded, we achieved conductive, functional yarns maintaining mechanical properties (strength and elongation) of electrospun polymer fibers. Because our composite methods do not depend on dispersion of conductive nanofillers in a polymer matrix, it is possible to obtain high electrical conductivity under small loading of carbon nanofillers. Our method enables producing various types of CNT-based composite yarns. Moreover, various functional materials based conductive yarns can be fabricated by our method. Thereby, more broad applications can be achieved through biscrolled composite yarns.

## Experimental

The styrene-ethylene-butylene-styrene (SEBS,  $M_w = \sim 118\,000\text{ g mol}^{-1}$ ), poly(vinylidene fluoride-*co*-hexafluoropropene) (PVDF-HFP,  $M_w = \sim 455\,000\text{ g mol}^{-1}$ ), chloroform, dimethylacetamide, acetone, and tetrahydrofuran were obtained from Aldrich (USA). Polyurethane (PU) was purchased from SMP Technologies Inc. (MM-4520, Japan). All polymers were used without further purification. The spinnable multiwalled nanotube forests were grown on a Si wafer using chemical vapor deposition.<sup>29</sup>

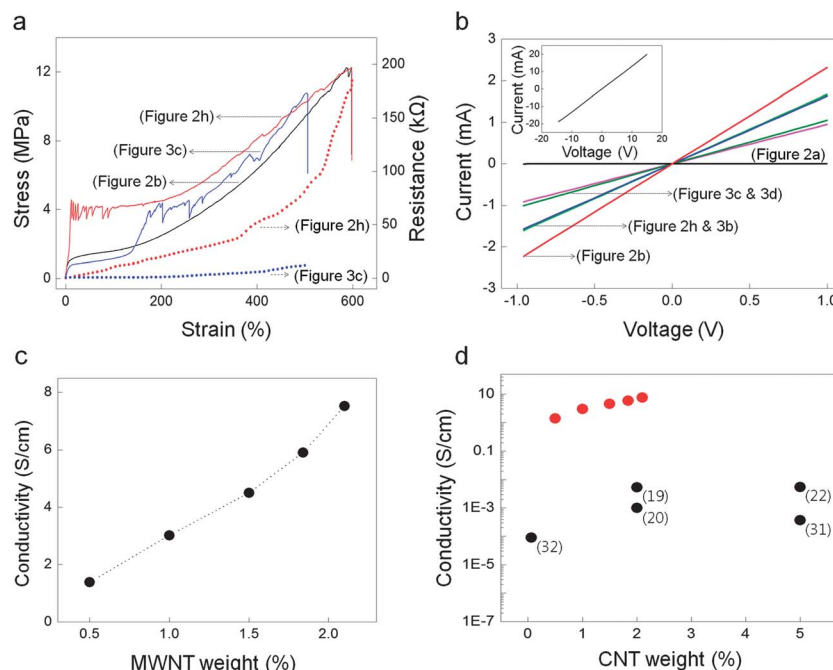


**Fig. 4** Mechanical and electrical properties of various types of AEF/CNT composite yarns. (a) Mechanical strength, elongation, and resistance of the polymer yarn (black), the bistructured composite yarn (red), and the regular winkled bistructured composite yarn (blue) (lines mean stress and dots mean resistance of the yarns). (b)  $I$ - $V$  characteristics for various types of AEF/CNT bistructured composite yarns (2 cm). The inset shows the range of dc linear ohmic behavior from -15 kV to 15 kV. (c) Electrical conductivity with increasing the number of CNT sheets. (d) Comparison of conductivity of previous composite fibers containing similar CNT loading research.<sup>19,20,22,32,33</sup>

SEBS, PVDF-HFP and PU for fabricating an AEF sheet were dissolved in chloroform (12 wt%), dimethylacetamide-acetone (3 : 7, 15 wt%) and tetrahydrofuran (15 wt%), respectively. The polymer solutions were stirred for 12 hours at room temperature. The setup for electrospinning is essentially the same as the conventional configuration except for the use of a collector containing a gap (~4 cm) in its middle. The polymer solutions were fed at a rate of 25  $\mu\text{L min}^{-1}$  using a syringe pump (KD Scientific, USA). A voltage of 17 kV was applied between a syringe needle (+10 kV) and the collector (-7 kV) using high-voltage DC power supplies (WooyongTECH, Korea). The distance between the syringe needle and the collector was 20 cm.

We used optical microscopy (SCB-2000) and field-emission scanning electron microscopy (FE SEM, Hitachi S4700) to study the morphology of yarns. SEM was operated at an accelerating voltage of 1 and 15 kV. The yarn tensile properties were measured using an Instron 5900 testing machine of Instron Corporation with load cell 250 N and the cross-head speed at 2 mm  $\text{min}^{-1}$ . And the  $I$ - $V$  curve of yarns was measured using a source meter (keithley 2650).

## Acknowledgements

This work was supported by the Creative Research Initiative Center for Bio-Artificial Muscle of the Ministry of Science, ICT & Future Planning (MSIP), the Industrial Strategic Technology Development Program (10038599), and the MSIP-US Air Force Cooperation Program (2013K1A3A1A32035592) in Korea and Air Force Grant AOARD-10-4067, Air Force Office of Scientific

Research grant FA9550-09-1-0537, and Robert A. Welch Foundation grant AT-0029 in the USA.

## Notes and references

- 1 Y. Dzenis, *Science*, 2004, **304**, 1917.
- 2 S. Agarwal, J. H. Wendorff and A. Greiner, *Adv. Mater.*, 2009, **21**, 3343.
- 3 I.-D. Kim, J.-M. Hong, B. H. Lee, D. Y. Kim, E.-K. Jeon, D.-K. Choi and D.-J. Yang, *Appl. Phys. Lett.*, 2007, **91**, 163109.
- 4 M. M. Demir, M. A. Gulgun, Y. Z. Menceoglu, B. Erman, S. S. Abramchuk, E. E. Makhaeva, A. R. Khokhlov, V. G. Matveeva and M. G. Sulman, *Macromolecules*, 2004, **37**, 1787.
- 5 H.-S. Park and Y. O. Park, *Korean J. Chem. Eng.*, 2005, **22**, 165.
- 6 S. Lee and S. K. Obendorf, *J. Appl. Polym. Sci.*, 2006, **102**, 3430.
- 7 M. Spasova, N. Manolova, M. Naydenov, J. Kuzmanova and I. Rashkov, *J. Bioact. Compat. Polym.*, 2012, **26**, 48.
- 8 Y. Zhang, X. He, J. Li, Z. Miao and F. Huang, *Sens. Actuators, B*, 2008, **132**, 67.
- 9 A. F. Lotus, S. Bhargava, E. T. Bender, E. A. Evans, R. D. Ramsier, D. H. Reneker and G. G. Chase, *J. Appl. Phys.*, 2009, **106**, 014303.
- 10 G. N. S. Vijayakumar, S. Devashankar, M. Rathnakumari and P. Sureshkumar, *J. Alloys Compd.*, 2010, **507**, 225.
- 11 D. Li and Y. Xia, *Adv. Mater.*, 2004, **16**, 1151.
- 12 M. K. Shin, S. I. Kim, S. J. Kim, S. Y. Park, Y. H. Hyun, Y. Lee, K. E. Lee, S.-S. Han, D.-P. Jang, Y.-B. Kim, Z.-H. Cho, I. So and G. M. Spinks, *Langmuir*, 2008, **24**, 12107.

- 13 N. Chanunpanich and H. Byun, *J. Appl. Polym. Sci.*, 2007, **106**, 3648.
- 14 X. Wang, K. Zhang, M. Zhu, H. Yu, Z. Zhou, Y. Chen and B. S. Hsiao, *Polymer*, 2008, **49**, 2755.
- 15 M. K. Shin, S. I. Kim, S. J. Kim, S.-K. Kim, H. Lee and G. M. Spinks, *Appl. Phys. Lett.*, 2006, **89**, 231929.
- 16 Z.-M. Huang, Y.-Z. Zhang, M. Kotaki and S. Ramakrishna, *Compos. Sci. Technol.*, 2003, **63**, 2223.
- 17 I. S. Chronakis, S. Grapenson and A. Jakob, *Polymer*, 2006, **47**, 1597.
- 18 X.-S. Wang, H.-P. Tang, X.-D. Li and X. Hua, *Int. J. Mol. Sci.*, 2009, **10**, 5527.
- 19 B. Sundaray, V. Subramanian, T. S. Natarajan and K. Krishnamurthy, *Appl. Phys. Lett.*, 2006, **88**, 143114.
- 20 S. Imaizumi, H. Matsumoto, Y. Konosu, K. Tsuboi, M. Minagawa, A. Tanioka, K. Koziol and A. Windle, *ACS Appl. Mater. Interfaces*, 2011, **3**, 469.
- 21 J. Hwang, J. Muth and T. Ghosh, *J. Appl. Polym. Sci.*, 2007, **104**, 2410.
- 22 S. Mazinani, A. Ajji and C. Dubois, *Polymer*, 2009, **50**, 3329.
- 23 M. T. Hunley, P. Pötschke and T. E. Long, *Macromol. Rapid Commun.*, 2009, **30**, 2102.
- 24 H. Hou, J. J. Ge, J. Zeng, Q. Li, D. H. Reneker, A. Greiner and S. Z. D. Cheng, *Chem. Mater.*, 2005, **17**, 967.
- 25 M. Naebe, T. Lin and X. Wang, in *Nanofibers*, ed. A. Kumar, Sciyo, INTECH, Croatia, 2010, vol. 1, ch. 16.
- 26 M. D. Lima, S. Fang, X. Lepró, C. Lewix, R. Ovalle-Robles, J. Carretero-González, E. Castillo-Martínez, M. E. Kozlov, J. Oh, N. Rawat, C. S. Haines, M. H. Haque, V. Aare, S. Stoughton, A. A. Zakhidov and R. H. Baughman, *Science*, 2011, **331**, 51.
- 27 M. Zhang, S. Fang, A. A. Zakhidov, S. B. lee, A. E. Aliev, C. D. Williams, K. R. Atkinson and R. H. Baughman, *Science*, 2005, **309**, 1215.
- 28 D. Li, Y. Wang and Y. Xia, *Nano Lett.*, 2003, **3**, 1167.
- 29 M. Zhang, K. R. Atkinson and R. H. Baughman, *Science*, 2004, **306**, 1358.
- 30 I. J. Beyerlein, P. K. Porwal, Y. T. Zhu, K. Hu and X. F. Xu, *Nanotechnology*, 2009, **20**, 485702.
- 31 M. T. Byrne and Y. K. Gun'ko, *Adv. Mater.*, 2010, **22**, 1672.
- 32 S. Mazinani, A. Ajji and C. Dubois, *J. Polym. Sci., Part B: Polym. Phys.*, 2010, **48**, 2052.
- 33 Z. M. Mahdiah, V. Mottaghitalab, N. Piri and A. K. Haghi, *Korean J. Chem. Eng.*, 2012, **29**, 111.